materials

MDPI

Article

Investigation of CO_2 Adsorption on Avocado Stone-Derived Activated Carbon Obtained through NaOH Treatment

Joanna Siemak [1], Rafał J. Wróbel [1], Jakub Pęksiński [2] and Beata Michalkiewicz [1,*]

[1] Department of Catalytic and Sorbent Materials Engineering, Faculty of Chemical Technology and Engineering, West Pomeranian University of Technology in Szczecin, Piastów Ave. 42, 71-065 Szczecin, Poland; joanna.siemak@zut.edu.pl (J.S.); rafal.wrobel@zut.edu.pl (R.J.W.)

[2] Faculty of Electrical Engineering, West Pomeranian University of Technology, 26 Kwietnia St. 10, 71-126 Szczecin, Poland; jpeksinski@zut.edu.pl

* Correspondence: beata.michalkiewicz@zut.edu.pl; Tel.: +48-91-449-4096; Fax: +48-91-449-4247

Abstract: Activated carbons were prepared from avocado stone through NaOH activation and subsequent carbonization. The following textural parameters were achieved: specific surface area: 817–1172 m^2/g, total pore volume: 0.538–0.691 cm^3/g, micropore volume 0.259–0.375 cm^3/g. The well-developed microporosity resulted in a good CO_2 adsorption value of 5.9 mmol/g at a temperature of 0 °C and 1 bar and selectivity over nitrogen for flue gas simulation. The activated carbons were investigated using nitrogen sorption at −196 °C, CO_2 sorption, X-ray diffraction, and SEM. It was found that the adsorption data were more in line with the Sips model. The isosteric heat of adsorption for the best sorbent was calculated. It was found that the isosteric heat of adsorption changed in the range of 25 to 40 kJ/mol depending on the surface coverage. The novelty of the work is the production of highly microporous activated carbons from avocado stones with high CO_2 adsorption. Before now, the activation of avocado stones using NaOH had never been described.

Keywords: CO_2 adsorption; carbon capture; avocado stone; activated carbons; selectivity

Citation: Siemak, J.; Wróbel, R.J.; Pęksiński, J.; Michalkiewicz, B. Investigation of CO_2 Adsorption on Avocado Stone-Derived Activated Carbon Obtained through NaOH Treatment. *Materials* **2023**, *16*, 4390. https://doi.org/10.3390/ma16124390

Academic Editor: Wen-Tien Tsai

Received: 15 May 2023
Revised: 9 June 2023
Accepted: 13 June 2023
Published: 14 June 2023

1. Introduction

Statistically, avocados are experiencing heightened demand, as substantiated by empirical evidence derived from comprehensive analyses of avocado production and harvesting regions. The world's avocado production reached 1.5×10^6 t in 1980, and in 2021, it reached 8.6×10^6 t [1]. The harvest area is also growing from one year to another. In 1980, the harvest area of avocados was equal to 180,000 hectares, and it was 858,000 hectares in 2021. In the future, a potential increasing demand will be observed. The world's biggest avocado producer is Mexico (2,442,945 t in 2021). The second and third biggest avocado producers in the world are Colombia (979,618 t in 2021) and Peru (777,096 t in 2021)

Commercial applications exclusively utilize the avocado pulp, disregarding any practical use for other elements of the fruit, such as the stone and peel, resulting in their disposal through landfill. Avocado stones, which account for approximately 26% of the fruit's total weight, are generated in significant quantities at centralized avocado transformation plants [2]. Despite their substantial starch content, the stones cannot be utilized as livestock feed due to their elevated polyphenol concentration, which imparts a bitter taste and may pose toxicity risks at high levels. In Mexico, 5% of produced avocado was destined for processing (primarily for guacamole), yielding 20,000 t of waste [3]. One way to utilize avocado waste may be the production of an economical and eco-friendly adsorbent material. However, there has been insufficient recognition of its potential as an adsorbent and precursor for the production of activated carbon [3].

Emerging research highlights the successful utilization of avocado waste as a cleaner and more sustainable raw material in the creation of adsorbents for wastewater treatment.

A method for producing activated carbons through activation with H_3PO_4 within the temperature range of 800 to 1000 °C was detailed [4]. The resulting material, which exhibited the highest adsorption capacity for blue 41 dye, had a relatively low surface area of 143 m^2/g and a low pore volume of 0.073 cm^3/g.

Sulfuric acid was employed as an activating agent in the synthesis of activated carbons from avocado stones, utilizing a temperature of 100 °C [5]. The resulting material exhibited a low specific surface area of 14 m^2/g and a low pore volume of 0.0323 cm^3/g and was utilized for the adsorption of Cr(VI) ions from aqueous solutions.

In one study, avocado stones were applied for activated carbon production for phenol removal from water [6]. The physical activation by CO_2 was performed at a temperature of 900 °C. The obtained activated carbon showed a low specific surface area (206 m^2/g) and low porosity.

In another study, $ZnCl_2$ was used as an activator in a microwave oven [7] for activated carbon production from avocado stones for resorcinol and 3-aminophenol removal from aqueous solutions. The low porosity of the obtained materials was identified (volume of mesopores: 0.325 cm^3/g and micropores: 0.119 cm^3/g).

The production of activated carbons from avocado stones through carbonization in nitrogen or carbon dioxide at 600–1000 °C has been presented [8]. The obtained materials exhibited low specific surface area (52–300 m^2/g) and low pore volume (0.051–0.172 cm^3/g), especially micropores (0.019–0.122 cm^3/g). Such properties allowed the use of these activated carbons as sorbents of fluorine ions from aqueous solutions.

All the activated carbons produced from avocado stones exhibited low porosity and were promising sorbent for wastewater. The adsorption of gases over activated carbons produced from avocado stones has not been described before. It was proven that high CO_2 adsorption requires highly microporous sorbents [9–11].

Activated carbon production has employed physical methods (thermal, steam) or alkalines (KOH, NaOH), acids (HCl, HNO_3, H_2SO_4, H_3PO_4), and other activating agents (O_3, H_2O_2, K_2CO_3, $ZnCl_2$, $FeCl_3$) [12]. KOH [13–16] was the most often employed, while the others have been less frequently applied.

NaOH was recently used by research groups as an activation agent. Zhu and Kolar [17] and Cazetta et al. [18] reported that KOH performed very well in terms of the adsorption of p–cresol and methylene blue, respectively. Martins et al. [19] described activated carbon synthesis using NaOH. They demonstrated high surface area and the presence of basic functional groups on the surface. Tan et al. [20] utilized NaOH for the modification of commercial activated carbon to improve their CO_2 capture. The increase in CO_2 adsorption was interpreted by the changes in morphology and replacing acid groups with Na^+.

On the basis of the investigations described above, we hypothesized that using NaOH as an activating agent for avocado stones as a carbon source may be a good solution for efficient CO_2 sorbents. NaOH has never been used as an activating agent for avocado stones before.

Biomass, with the exception of avocado stones, has been successfully used to produce good CO_2 sorbents. Table 1 shows the CO_2 adsorption at a temperature of 0 °C and pressure of 1 bar achieved by other authors.

The objective of this study is to produce activated carbons from avocado stones and NaOH as an activating agent for CO_2 adsorption. As far as we know, there have been no studies in the literature that demonstrate the use of NaOH as an activating agent for creating activated carbons from avocado stones. The utilization of NaOH resulted in our obtaining activated carbons with high porosity, especially microporosity, which is essential for CO_2 adsorption. The application of activated carbon from avocado stones for CO_2 capture is also presented for the first time. A very high CO_2 adsorption value (qCO_{2_0C}) was achieved at a temperature of 0 °C and pressure 1 bar, namely 5.9 mmol/g. Compared to other researchers, this is one of the higher adsorption values.

Table 1. CO_2 adsorption at a temperature of 0 °C and pressure of 1 bar.

Biomass	qCO_{2_0C}	References
	(mmol/g)	
rice husk	5.83	[21]
walnut shell	5.22	[22]
palm sheath	5.28	[23]
Amazonian nutshells	5.13	[24]
lignocellulose	5.20	[25]
peanut shells	5.20	[26]
pomegranate peels	3.90	[26]
birch	4.50	[27]
coconut shell	6.04	[28]
corn cobs	2.70	[26]

2. Materials and Methods

Activated carbon was prepared from avocado stone. NaOH was applied as activating agent. The temperature of carbonization ranged from 750 to 850 °C. The sodium residues were removed during washing with water. Soaking in 1 M HCl lasted 15 min. The synthesis details are shown in Scheme 1.

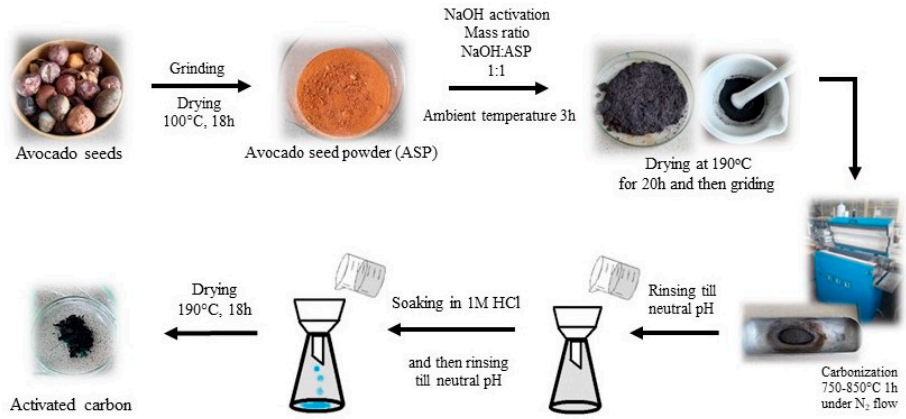

Scheme 1. The synthesis scheme of avocado stone-derived activated carbon activated by NaOH.

We collected avocado stones, dried them, and ground them to a powder. On the basis of EDX (Spectrometer XPS, SES-2002, Scienta Scientific AB, Uppsala, Sweden, 2002) of dried powdered material, we can conclude that the precursor was carbonaceous material containing about 5% K (Figure S1). Cr was identified because in order to make these measurements, the sample had to be covered by Cr.

The specific surface area (SSA), total pore volume (V_{tot}), micropore volume (V_{micro}), pore size distribution, and the highest pore size maxD estimated using the N_2 adsorption for which the total pore volume was determined were measured on a ASAP Sorption Surface Area and Pore Size Analyzer (ASAP 2460, Micrometrics, Norcross, GA, USA, 2018). Before the measurements, samples were degassed at a temperature of 250 °C for 16 h. Sorption isotherms were investigated at −196 °C. SSAs were calculated based on the BET method. Micropore volume and pore size distribution were calculated through density functional theory using the carbon slit model. Pore volume was estimated on the basis of nitrogen volume adsorbed at the highest p/p_0.

An X'Pert–PRO, Panalytical, Almelo, The Netherlands, 2012, X-ray diffractometer equipped with a copper source was employed for the XRD analysis. In each XRD scan, the scan rate was 1°/min with 2θ from 5 to 60°.

The field emission scanning electron microscopy images were acquired using a SU8020 Ultra-High Resolution Field Emission Scanning Electron Microscope; Hitachi Ltd., Tokyo, Japan, 2012, under 15 kV voltage.

A sorption analyzer ASAP Sorption Surface Area and Pore Size Analyzer (ASAP 2460, Micrometrics, Norcross, GA, USA, 2018) was also utilized to investigate the nitrogen and carbon dioxide uptake at a temperature of 0 and 20 °C. The adsorption isotherms were obtained.

3. Results and Discussion

Nitrogen adsorption–desorption isotherms are presented in Figure 1. The sorption isotherms display I and IV combined types according to the IUPAC [29] classification, meaning that the activated carbons were micro–mesoporous materials.

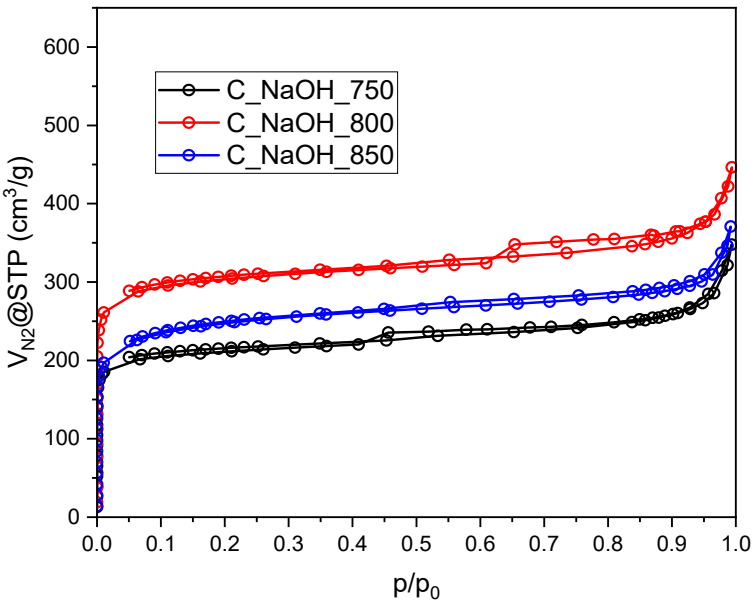

Figure 1. Nitrogen sorption isotherms measured at −196 °C for avocado stone-derived activated carbon activated by NaOH.

The significant N_2 uptake at a relative pressure (p/p_0) below 0.01 is evident and proved narrow micropore presence. The capillary condensation step at a relative pressure range above 0.55 is present, which demonstrates the presence of mesopores.

According to UPAC, pores are classified into the following groups: micropores < 2.0, mesopores in the range of 2.0–50 nm, and macropores > 50 nm [30]. Some authors subdivide micropores into two groups: narrow micropores or ultramicro pores < 0.7 nm and supermicropores in the range of 0.7 to 2.0 nm [30].

The pore size distribution (Figure 2) of all samples exhibited similar pore structure. The narrow micropores were predominant in all the activated carbons. Textural parameters are listed in Table 2. For all samples, the micropores accounted for about 50% of the pore volume. The highest specific surface area, pore volume, and micropore volume were obtained for C_NaOH_800.

This material also exhibited the highest volume of pores smaller than 1 nm. Activated carbon produced at 800 °C was the most porous material. At lower temperatures, the porous structure was not able to develop well. At higher temperatures, the structure was destroyed to some extent.

Figure 3 shows SEM images of avocado stone-derived activated carbon obtained through NaOH treatment. Visual observation of the material's surface revealed the developed surface and macropores that, deeper into the material, may branch into mesopores and finally into micropores.

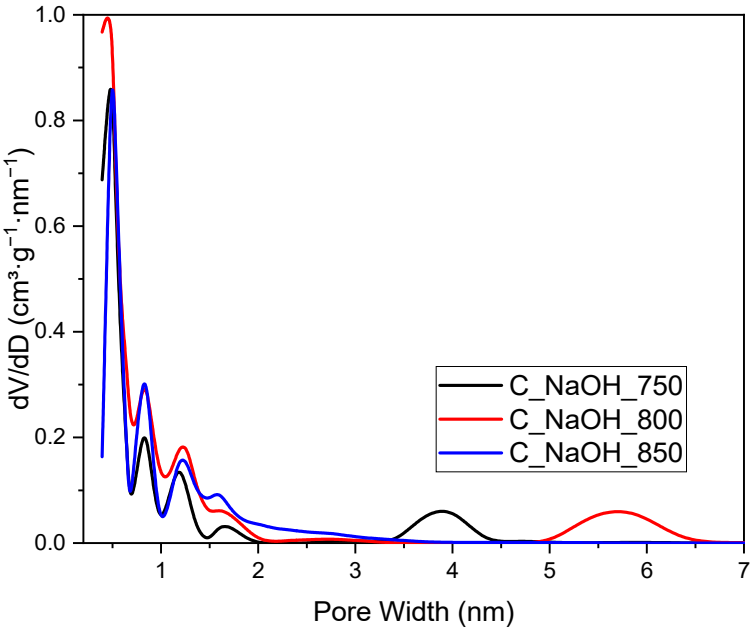

Figure 2. Pore volume size distribution calculated using DFT method for avocado stone-derived activated carbon activated by NaOH.

Table 2. Textural parameters and CO_2 adsorption values of avocado stone-derived activated carbon activated by NaOH.

AC	SSA	V_{tot}	V_{micro}	maxD	q_{CO2_0C}
	[m^2/g]	[cm^3/g]	cm^3/g	[nm]	[mmol/g]
C_NaOH_750	817	0.538	0.259	297	4.6
C_NaOH_800	1172	0.691	0.375	312	5.9
C_NaOH_850	918	0.574	0.295	241	3.7

XRD patterns of avocado stone-derived activated carbon activated by NaOH are shown in Figure 4. Two broad signals at about 22 and 44° are seen. The first peak is attributed to the surface of the turbostratic carbon [31]. The second one is characteristic of the longitudinal dimension, the so-called aromatic sheets [32]. Based on the shapes of the peaks, one can conclude that the avocado stone-derived activated carbons were primarily amorphous [33]. The increase in diffraction intensity at $2\theta < 10°$ confirms the development of micropores and mesopores [34,35]. Apart from broad carbon signals, no other peaks were observed. It can be assumed that sodium was wholly removed from the samples. The EDX results confirmed the absence of Na (Figure S1).

Figure 5 presents the carbon dioxide adsorption isotherms at 0 °C. The highest CO_2 adsorption (5.9 mmol/g) was achieved over C_NaOH_800. This material exhibited the highest specific surface area, total pore volume, and micropore volume. The importance of the textural parameters for high CO_2 adsorption was emphasized by many authors [9,36,37]. In particular, pores with a diameter of less than 1 nm are considered crucial for CO_2 adsorption [38–41]. The CO_2 adsorption values at the temperature of 0 °C and pressure of 1 bar (q_{CO2_0C}) are presented in Table 2.

In order to calculate the CO_2 adsorption selectivity over N_2 at the temperature of 20 °C, CO_2 and N_2 adsorption measurements over C_NaOH_800 were performed at 20 °C. The results of CO_2 and N_2 adsorption at 20 °C are presented in Figure 6. The CO_2 adsorption at the temperature of 20 °C and pressure of 1 bar was equal to 4.3 mmol/g. The decrease in CO_2 adsorption by increasing the temperature is due to physisorption. To clearly show the effect of CO_2 adsorption temperature over C_NaOH_800 on CO_2 adsorption value, Figure S2 was drawn.

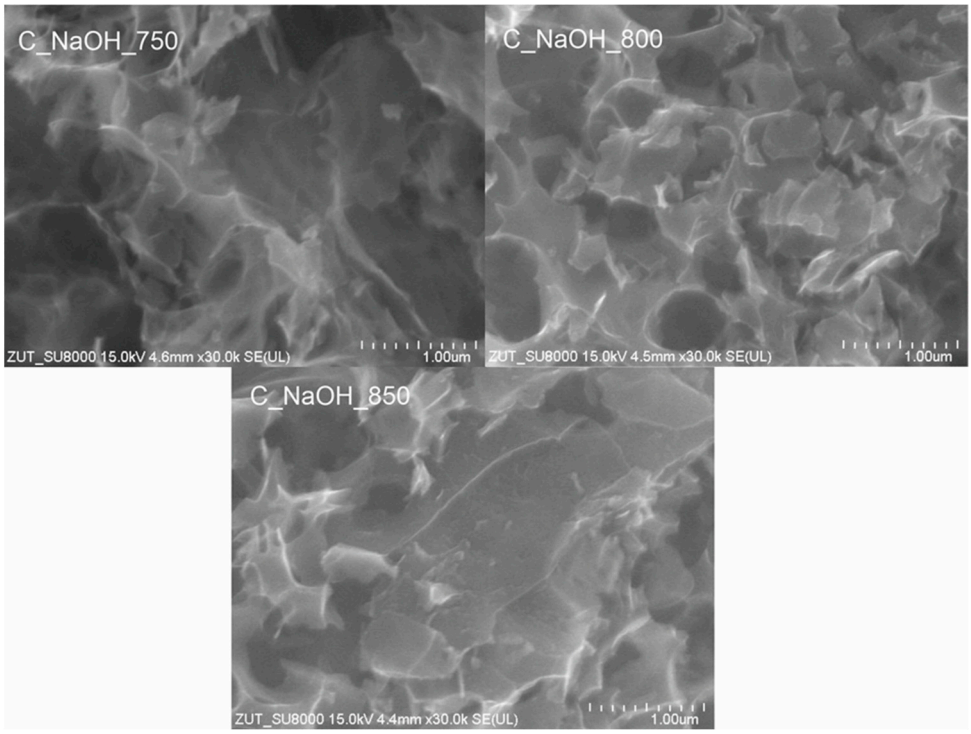

Figure 3. SEM images of avocado stone-derived activated carbon activated by NaOH.

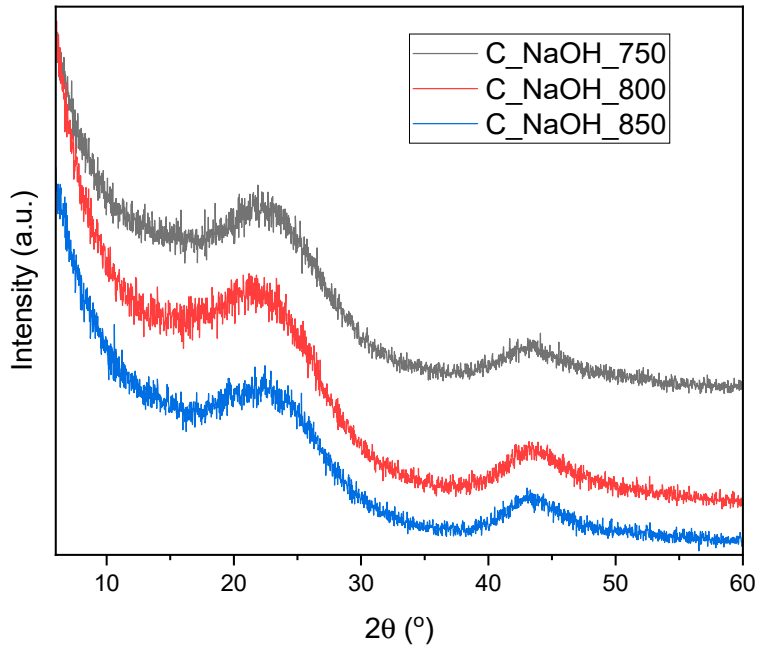

Figure 4. XRD pattern of avocado stone-derived activated carbons activated by NaOH.

The CO_2 and N_2 adsorption data were fitted by the following adsorption isotherm equations: Langmuir, Freundlich, Sips. These equations were described in [42,43]. The data were more in line with the Sips model. The Sips model is given by the equation:

$$q = \frac{q_m \cdot b \cdot p^n}{1 + b \cdot p^n}$$

where:

q—gas equilibrium adsorption at pressure p;

p—equilibrium pressure;
q_m—saturation capacity;
b—equilibrium constant;
n—exponential parameter representing the heterogeneity of the material.

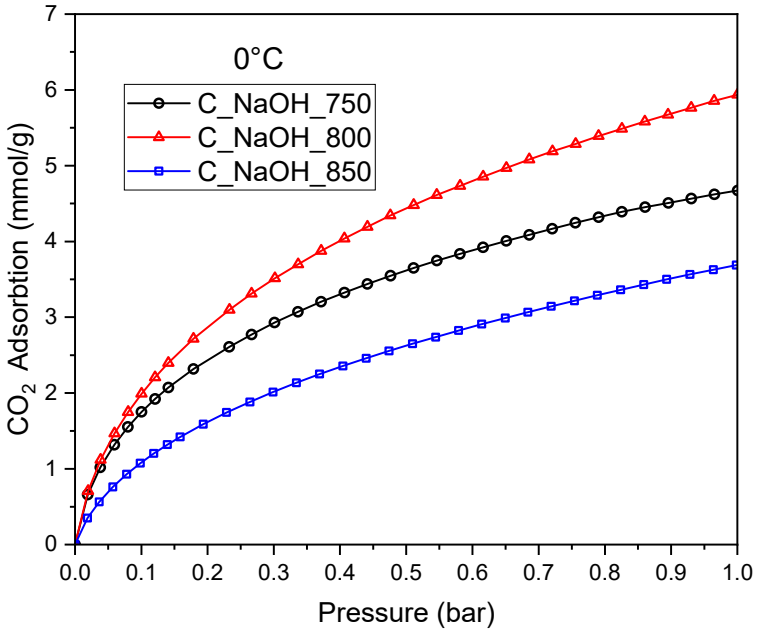

Figure 5. CO_2 adsorption isotherms at a temperature of 0 °C over avocado stone-derived activated carbon activated by NaOH. The points represent experimental data. The lines were drawn using the Sips model.

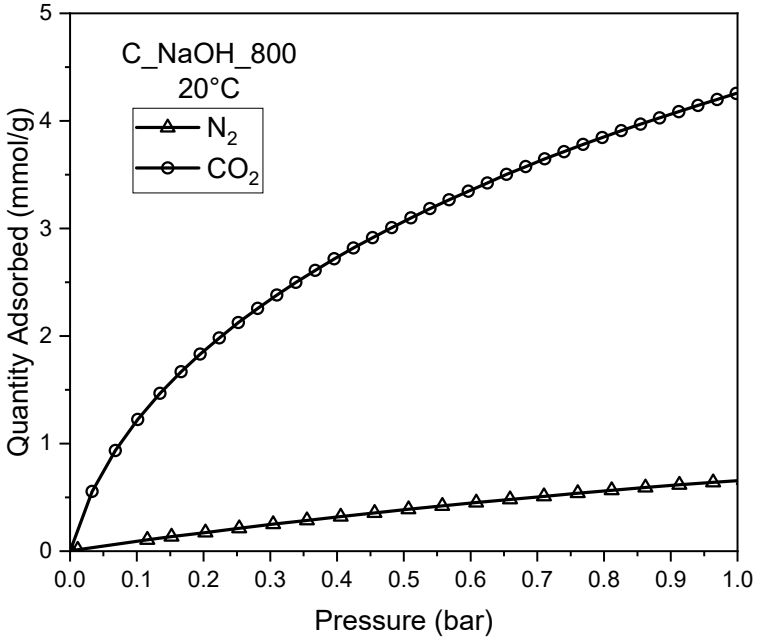

Figure 6. CO_2 and N_2 adsorption isotherms at a temperature of 20 °C over C_NaOH_800. The points represent experimental data. The lines were drawn using the Sips model.

The fitting accuracy of the models was judged using the least-squares method (LSM), which is most commonly used as an error function [44]:

$$LSM = \sum_{i=1}^{N} (q_{e,o} - q_{e,z})^2$$

where:

$q_{e,o}$—theoretical adsorption capacity calculated from the model;
$q_{e,z}$—adsorption capacity determined experimentally;
N—total number of measurements.

The fitting parameters of the Sips model are displayed in Table 3.

Table 3. The Sips model parameters and standard error calculated based on experimental data of CO_2 and N_2 adsorption.

AC	Temp.	q_m	b	n	*LSM*
	[°C]	[mmol/g]	[bar^{-1}]		
		Carbon dioxide			
C_NaOH_750	0	10.26	0.84	0.62	4×10^{-3}
C_NaOH_800	0	14.46	0.69	0.64	7×10^{-3}
C_NaOH_850	0	12.21	0.43	0.65	4×10^{-3}
C_NaOH_800	20	10.59	0.67	0.72	15×10^{-3}
		Nitrogen			
C_NaOH_800	20	2.34	0.39	0.99	3×10^{-5}

The saturation capacity becomes lower when the temperature becomes higher, which confirms the physical adsorption. The n values are higher than 0.5, which suggests homogeneity of the surface for CO_2 and N_2 adsorption.

Judgment as to the physical or chemical mechanism of adsorption should only be made on the basis of the best fit model. However, the results obtained using the Langmuir model were similar. The value of the saturation capacity of the Langmuir model (q_{mL}) for the temperature of 0 °C was also higher than for the temperature of 20 °C for C_NaOH_800. The q_{mL} values confirmed the physical nature of CO_2 adsorption. The Freundlich model does not describe a limit in adsorption capacity. In this case, the adsorption theoretically may be infinite, so a conclusion similar to the Sips and Langmuir models about the nature of adsorption cannot be drawn.

In order to calculate the selectivity, the Sips model and ideal adsorbed solution theory (IAST) proposed for the first time by Myers and Praunitz [44] were utilized. The IAST was applied to calculate the selectivity of carbon dioxide over nitrogen at 20 °C. The IAST is universally utilized for anticipating the selectivity from mixed gas adsorption isotherms compared to pure component isotherms with a reasonable accuracy for different gas mixtures. The precision of the IAST method was proved for the adsorption of various gas systems over various sorbents [45,46].

The selectivity of gas 1 over gas 2 is possible to predict based on single adsorption isotherms of gas 1 and gas 2:

$$S_{(g1)} = \frac{\frac{x_{g1}}{y_{g1}}}{\frac{x_{g2}}{y_{g2}}}$$

where:

x_{g1} (x_{g2})—the molar fractions of gas 1/gas 2 ($g1/g2$) in the adsorbed phase;
y_{g1}, (y_{g2})—the molar fractions of gas 1/gas 2 ($g1/g2$) in the bulk phase.

The selectivity calculations were made for equimolar mixtures. The results are presented in Figure 7.

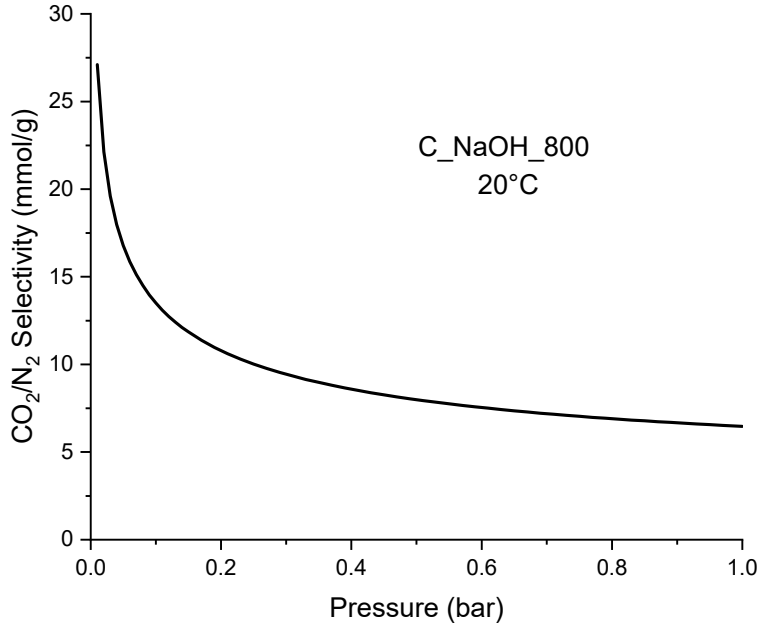

Figure 7. The selectivity of CO_2 adsorption for the equimolar mixture of CO_2 and N_2 at 20 °C.

The selectivity of CO_2 ranged from 27 to 6 at pressures from 0.01 to 1. The course of the curve is typical for CO_2 over N_2 selectivity [47–49].

For the CO_2 captured from flue gas, the selectivity for a mixture containing 15% CO_2 is essential. The selectivity of CO_2 over N_2 for 15% CO_2 content was calculated based on IAST theory according to the following equation:

$$S_{(CO_2@15bar)} = \frac{q_{CO_2@15bar}}{q_{N_2@85bar}} \cdot \frac{0.85}{0.15}$$

The selectivity for CO_2 content typical for flue gas was relatively high and was equal to 15, indicating its potential in post-combustion CO_2 capture.

The isosteric heat of adsorption Q_{iso} is significant for the evaluation of sorbents. Q_{iso} gives knowledge about the changes in the enthalpy during the progress of CO_2 adsorption. It is a measure of the interaction of adsorbate molecules and adsorbent atoms. The isosteric heat of adsorption is expressed by the Clausius–Clapeyron equation:

$$Q_{iso} = -R \left(\frac{\partial \ln(p)}{\partial \left(\frac{1}{T} \right)} \right)_{\theta}$$

Q_{iso} is the isosteric heat of adsorption at constant surface coverage (kJ/mol), R is the gas constant (J/mol·K), and θ is the surface coverage degree.

After differentiation of the above equation, a linear equation (adsorption isostere) is obtained:

$$\ln(p)_{\theta} = -\frac{Q_{iso}}{R} \frac{1}{T} + C$$

Sips equations for temperatures 0 and 20 °C were utilized to calculate the pressure for every value of C_NaOH_800 surface coverage degree. Only two temperatures were applied for the isosteric heat of adsorption calculation, but in [50], it was proven that the results obtained for two and for five temperatures were nearly identical. Adsorption isosteres with different surface coverage are presented in Figure S5.

The linear form was utilized to calculate the isosteric heat of adsorption for various degrees of coverage of the C_NaOH_800 surface with CO_2 particles. On the basis of the

slope (S) of the line, the isosteric head of adsorption was calculated for every surface coverage degree.

$$S = -\frac{Q_{iso}}{R}$$

The isosteric heat of adsorption as a function of surface coverage is shown in Figure 8. The Q_{iso} change is in the range of 25 to 40 kJ/mol, which proves physisorption [51]. The high initial isosteric heat of adsorption is likely caused by stronger Van der Waals' forces between the carbon surface and CO_2 molecules at coverage close to 0. With the increase in surface coverage, the heat of adsorption decreases because of the continuous occupation of "CO_2-philic" active sites [52].

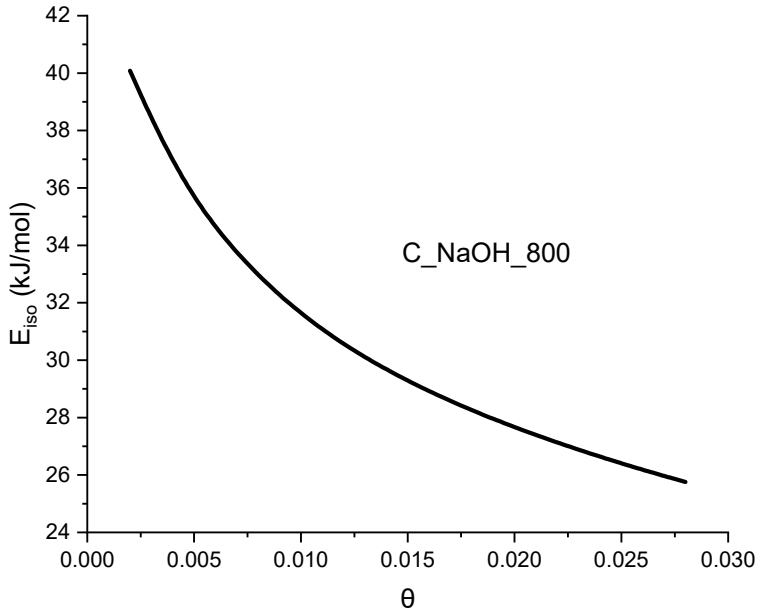

Figure 8. Isosteric heat of adsorption as a function of C_NaOH_800 surface coverage.

There are two common checkpoints used to determine if adsorption is physical or chemical:

- the changes in the gas absorption values (and the saturation capacity) with the increase in the temperature;
- the isosteric heat of adsorption value.

If the gas absorption values (and the saturation capacity) decrease with the increase in the temperature, physical adsorption has to be postulated. The heat of adsorption in physisorption lies in the range of 10–40 kJ/mol. If it is higher, the chemical reaction between the gas and surface can be assumed. We showed that the adsorption of CO_2 values at the same pressure, as well as the saturation capacity, decreased with the increase in the temperature, and the isosteric head of adsorption was lower than 40 kJ/mol. These facts proved that physisorption took place.

4. Conclusions

The carbonization temperature of avocado stone-derived activated carbon activated by NaOH substantially influenced the porosity of the resultant materials. For the production of suitable adsorbents for CO_2, a relatively moderate activation temperature (800 °C) is required. Carbonization at 800 °C provided a high volume of small micropores (size < 1 nm), which is essential for CO_2 adsorption.

Activated carbon produced through the NaOH activation of avocado stones and carbonization at 800 °C showed high CO_2 adsorption (5.9 mmol/g at 0 °C, 1 bar). The Sips isotherm model was found to be the one fitting the adsorption data the best. On the basis of the adsorption, values change with the temperature increase. With the saturation

capacity of the Sips equation and the isosteric heat of adsorption, the physisorption of CO_2 was found over avocado stone-derived activated carbon activated by NaOH.

A very high CO_2 adsorption value at 0 °C and pressure of 1 bar was achieved: 5.9 mmol/g. Compared to other researchers, this is one of the higher adsorption values.

Supplementary Materials: The following supporting information can be downloaded at: https://www.mdpi.com/article/10.3390/ma16124390/s1, Figure S1: EDX spectra; Figure S2: CO_2 adsorption isotherms at a temperature of 0 °C and 20 °C over C_NaOH_800. The points represent experimental data. The lines were drawn using the Sips model; Figure S3: CO_2 adsorption isotherms at a temperature of 0 °C and 20 °C over C_NaOH_800. The points represent experimental data. The lines were drawn using the Langmuir model; Figure S4: CO_2 adsorption isotherms at a temperature of 0 °C and 20 °C over C_NaOH_800. The points represent experimental data. The lines were drawn using the Freundlich model; Figure S5: Adsorption isosteres with different surface coverage; Table S1: The Langmuir model parameters and standard error calculated based on experimental data of CO_2 for C_NaOH_800; Table S2: The Freundlich model parameters and standard error calculated based on experimental data of CO_2 for C_NaOH_800.

Author Contributions: Conceptualization, J.S. and B.M.; methodology, J.S. and B.M.; investigation, J.S. and R.J.W.; data curation, J.S. and J.P.; writing—original draft preparation, J.S. and B.M.; writing—review and editing, J.S. and B.M.; visualization, J.S.; supervision, B.M.; funding acquisition, J.P. All authors have read and agreed to the published version of the manuscript.

Funding: This research received no external funding.

Institutional Review Board Statement: Not applicable.

Informed Consent Statement: Not applicable.

Data Availability Statement: The data presented in this study are available upon request from the corresponding author.

Conflicts of Interest: The authors declare no conflict of interest.

References

1. FAOSTAT. Agriculture Data. 2021. Available online: https://www.fao.org/faostat/en/#data/QCL (accessed on 5 June 2023).
2. Domínguez, M.P.; Araus, K.; Bonert, P.; Sánchez, F.; San Miguel, G.; Toledo, M. *The Avocado and Its Waste: An Approach of Fuel Potential/Application*; Springer: Cham, Switzerland, 2014; pp. 199–223.
3. Perea-Moreno, A.-J.; Aguilera-Ureña, M.-J.; Manzano-Agugliaro, F. Fuel Properties of Avocado Stone. *Fuel* **2016**, *186*, 358–364. [CrossRef]
4. Elizalde-González, M.P.; Mattusch, J.; Peláez-Cid, A.A.; Wennrich, R. Characterization of Adsorbent Materials Prepared from Avocado Kernel Seeds: Natural, Activated and Carbonized Forms. *J. Anal. Appl. Pyrolysis* **2007**, *78*, 185–193. [CrossRef]
5. Bhaumik, M.; Choi, H.J.; Seopela, M.P.; McCrindle, R.I.; Maity, A. Highly Effective Removal of Toxic Cr(VI) from Wastewater Using Sulfuric Acid-Modified Avocado Seed. *Ind. Eng. Chem. Res.* **2014**, *53*, 1214–1224. [CrossRef]
6. Rodrigues, L.A.; da Silva, M.L.C.P.; Alvarez-Mendes, M.O.; dos Reis Coutinho, A.; Thim, G.P. Phenol Removal from Aqueous Solution by Activated Carbon Produced from Avocado Kernel Seeds. *Chem. Eng. J.* **2011**, *174*, 49–57. [CrossRef]
7. Leite, A.J.; Sophia, A.C.; Thue, P.S.; dos Reis, G.S.; Dias, S.L.; Lima, E.C.; Vaghetti, J.C.P.; Pavan, F.A.; de Alencar, W.S. Activated Carbon from Avocado Seeds for the Removal of Phenolic Compounds from Aqueous Solutions. *Desalin. Water Treat.* **2017**, *71*, 168–181. [CrossRef]
8. Salomón-Negrete, M.Á.; Reynel-Ávila, H.E.; Mendoza-Castillo, D.I.; Bonilla-Petriciolet, A.; Duran-Valle, C.J. Water Defluoridation with Avocado-Based Adsorbents: Synthesis, Physicochemical Characterization and Thermodynamic Studies. *J. Mol. Liq.* **2018**, *254*, 188–197. [CrossRef]
9. Serafin, J.; Kiełbasa, K.; Michalkiewicz, B. The New Tailored Nanoporous Carbons from the Common Polypody (*Polypodium vulgare*): The Role of Textural Properties for Enhanced CO_2 Adsorption. *Chem. Eng. J.* **2022**, *429*, 131751. [CrossRef]
10. Casco, M.E.; Martínez-Escandell, M.; Silvestre-Albero, J.; Rodríguez-Reinoso, F. Effect of the Porous Structure in Carbon Materials for CO_2 Capture at Atmospheric and High-Pressure. *Carbon* **2014**, *67*, 230–235. [CrossRef]
11. Deng, S.; Hu, B.; Chen, T.; Wang, B.; Huang, J.; Wang, Y.; Yu, G. Activated Carbons Prepared from Peanut Shell and Sunflower Seed Shell for High CO_2 Adsorption. *Adsorption* **2015**, *21*, 125–133. [CrossRef]
12. Jang, H.M.; Yoo, S.; Choi, Y.-K.; Park, S.; Kan, E. Adsorption Isotherm, Kinetic Modeling and Mechanism of Tetracycline on Pinus Taeda-Derived Activated Biochar. *Bioresour. Technol.* **2018**, *259*, 24–31. [CrossRef] [PubMed]
13. Teng, H.; Hsu, L.-Y. High-Porosity Carbons Prepared from Bituminous Coal with Potassium Hydroxide Activation. *Ind. Eng. Chem. Res.* **1999**, *38*, 2947–2953. [CrossRef]

14. Li, P.; Xing, C.; Qu, S.; Li, B.; Shen, W. Carbon Dioxide Capturing by Nitrogen-Doping Microporous Carbon. *ACS Sustain. Chem. Eng.* **2015**, *3*, 1434–1442. [CrossRef]
15. Silvestre-Albero, A.; Silvestre-Albero, J.; Martínez-Escandell, M.; Rodríguez-Reinoso, F. Micro/Mesoporous Activated Carbons Derived from Polyaniline: Promising Candidates for CO_2 Adsorption. *Ind. Eng. Chem. Res.* **2014**, *53*, 15398–15405. [CrossRef]
16. De Souza, L.K.C.; Wickramaratne, N.P.; Ello, A.S.; Costa, M.J.F.; da Costa, C.E.F.; Jaroniec, M. Enhancement of CO_2 Adsorption on Phenolic Resin-Based Mesoporous Carbons by KOH Activation. *Carbon* **2013**, *65*, 334–340. [CrossRef]
17. Zhu, Y.; Kolar, P. Investigation of Adsorption of *p*-Cresol on Coconut Shell-Derived Activated Carbon. *J. Taiwan Inst. Chem. Eng.* **2016**, *68*, 138–146. [CrossRef]
18. Cazetta, A.L.; Vargas, A.M.M.; Nogami, E.M.; Kunita, M.H.; Guilherme, M.R.; Martins, A.C.; Silva, T.L.; Moraes, J.C.G.; Almeida, V.C. NaOH-Activated Carbon of High Surface Area Produced from Coconut Shell: Kinetics and Equilibrium Studies from the Methylene Blue Adsorption. *Chem. Eng. J.* **2011**, *174*, 117–125. [CrossRef]
19. Martins, A.C.; Pezoti, O.; Cazetta, A.L.; Bedin, K.C.; Yamazaki, D.A.S.; Bandoch, G.F.G.; Asefa, T.; Visentainer, J.V.; Almeida, V.C. Removal of Tetracycline by NaOH-Activated Carbon Produced from Macadamia Nut Shells: Kinetic and Equilibrium Studies. *Chem. Eng. J.* **2015**, *260*, 291–299. [CrossRef]
20. Tan, Y.L.; Islam, M.A.; Asif, M.; Hameed, B.H. Adsorption of Carbon Dioxide by Sodium Hydroxide-Modified Granular Coconut Shell Activated Carbon in a Fixed Bed. *Energy* **2014**, *77*, 926–931. [CrossRef]
21. He, S.; Chen, G.; Xiao, H.; Shi, G.; Ruan, C.; Ma, Y.; Dai, H.; Yuan, B.; Chen, X.; Yang, X. Facile Preparation of N-Doped Activated Carbon Produced from Rice Husk for CO_2 Capture. *J. Colloid Interface Sci.* **2021**, *582*, 90–101. [CrossRef]
22. Yang, Z.; Zhang, G.; Xu, Y.; Zhao, P. One Step N-Doping and Activation of Biomass Carbon at Low Temperature through NaNH2: An Effective Approach to CO_2 Adsorbents. *J. CO_2 Util.* **2019**, *33*, 320–329. [CrossRef]
23. Zhang, Y.; Wei, Z.; Liu, X.; Liu, F.; Yan, Z.; Zhou, S.; Wang, J.; Deng, S. Synthesis of Palm Sheath Derived-Porous Carbon for Selective CO_2 Adsorption. *RSC Adv.* **2022**, *12*, 8592–8599. [CrossRef]
24. Serafin, J.; Ouzzine, M.; Cruz Junior, O.F.; Sreńscek-Nazzal, J. Preparation of Low-Cost Activated Carbons from Amazonian Nutshells for CO_2 Storage. *Biomass Bioenergy* **2021**, *144*, 105925. [CrossRef]
25. Parshetti, G.K.; Chowdhury, S.; Balasubramanian, R. Biomass Derived Low-Cost Microporous Adsorbents for Efficient CO_2 Capture. *Fuel* **2015**, *148*, 246–254. [CrossRef]
26. Mumtaz, H.; Farhan, M.; Amjad, M.; Riaz, F.; Kazim, A.H.; Sultan, M.; Farooq, M.; Mujtaba, M.A.; Hussain, I.; Imran, M.; et al. Biomass Waste Utilization for Adsorbent Preparation in CO_2 Capture and Sustainable Environment Applications. *Sustain. Energy Technol. Assess.* **2021**, *46*, 101288. [CrossRef]
27. Kishibayev, K.K.; Serafin, J.; Tokpayev, R.R.; Khavaza, T.N.; Atchabarova, A.A.; Abduakhytova, D.A.; Ibraimov, Z.T.; Sreńscek-Nazzal, J. Physical and Chemical Properties of Activated Carbon Synthesized from Plant Wastes and Shungite for CO_2 Capture. *J. Environ. Chem. Eng.* **2021**, *9*, 106798. [CrossRef]
28. Yang, J.; Yue, L.; Hu, X.; Wang, L.; Zhao, Y.; Lin, Y.; Sun, Y.; DaCosta, H.; Guo, L. Efficient CO_2 Capture by Porous Carbons Derived from Coconut Shell. *Energy Fuels* **2017**, *31*, 4287–4293. [CrossRef]
29. Sing, K.S.W. Reporting Physisorption Data for Gas/Solid Systems with Special Reference to the Determination of Surface Area and Porosity (Recommendations 1984). *Pure Appl. Chem.* **1985**, *57*, 603–619. [CrossRef]
30. Sing, K.S.W.; Everett, D.H.; Haul, R.A.W.; Moscou, L.; Pierotti, R.A.; Rouquerol, J.; Siemieniewska, T. Reporting Physisorption Data for Gas/Solid Systems. In *Handbook of Heterogeneous Catalysis*; Wiley-VCH Verlag GmbH & Co. KGaA: Weinheim, Germany, 2008.
31. Wang, D.; Liu, S.; Fang, G.; Geng, G.; Ma, J. From Trash to Treasure: Direct Transformation of Onion Husks into Three-Dimensional Interconnected Porous Carbon Frameworks for High-Performance Supercapacitors in Organic Electrolyte. *Electrochim. Acta* **2016**, *216*, 405–411. [CrossRef]
32. Wu, Z.; Tian, K.; Huang, T.; Hu, W.; Xie, F.; Wang, J.; Su, M.; Li, L. Hierarchically Porous Carbons Derived from Biomasses with Excellent Microwave Absorption Performance. *ACS Appl. Mater. Interfaces* **2018**, *10*, 11108–11115. [CrossRef]
33. Zhang, R.; Qiao, J.; Zhang, X.; Yang, Y.; Zheng, S.; Li, B.; Liu, W.; Liu, J.; Zeng, Z. Biomass-Derived Porous Carbon for Microwave Absorption. *Mater. Chem. Phys.* **2022**, *289*, 126437. [CrossRef]
34. Zhang, X.; Yan, Q.; Leng, W.; Li, J.; Zhang, J.; Cai, Z.; Hassan, E. Carbon Nanostructure of Kraft Lignin Thermally Treated at 500 to 1000 °C. *Materials.* **2017**, *10*, 975. [CrossRef] [PubMed]
35. Zhang, X.; Elsayed, I.; Song, X.; Shmulsky, R.; Hassan, E.B. Microporous Carbon Nanoflakes Derived from Biomass Cork Waste for CO_2 Capture. *Sci. Total Environ.* **2020**, *748*, 142465. [CrossRef] [PubMed]
36. Serafin, J.; Sreńscek-Nazzal, J.; Kamińska, A.; Paszkiewicz, O.; Michalkiewicz, B. Management of Surgical Mask Waste to Activated Carbons for CO_2 Capture. *J. CO_2 Util.* **2022**, *59*, 101970. [CrossRef]
37. Młodzik, J.; Sreńscek-Nazzal, J.; Narkiewicz, U.; Morawski, A.W.; Wróbel, R.J.; Michalkiewicz, B. Activated Carbons from Molasses as CO_2 Sorbents. *Acta Phys. Pol. A* **2016**, *129*, 402–404. [CrossRef]
38. Wickramaratne, N.P.; Jaroniec, M. Activated Carbon Spheres for CO_2 Adsorption. *ACS Appl. Mater. Interfaces* **2013**, *5*, 1849–1855. [CrossRef]
39. Deng, S.; Wei, H.; Chen, T.; Wang, B.; Huang, J.; Yu, G. Superior CO_2 Adsorption on Pine Nut Shell-Derived Activated Carbons and the Effective Micropores at Different Temperatures. *Chem. Eng. J.* **2014**, *253*, 46–54. [CrossRef]
40. Wei, H.; Deng, S.; Hu, B.; Chen, Z.; Wang, B.; Huang, J.; Yu, G. Granular Bamboo-Derived Activated Carbon for High CO_2 Adsorption: The Dominant Role of Narrow Micropores. *ChemSusChem* **2012**, *5*, 2354–2360. [CrossRef]

41. Presser, V.; McDonough, J.; Yeon, S.-H.; Gogotsi, Y. Effect of Pore Size on Carbon Dioxide Sorption by Carbide Derived Carbon. *Energy Environ. Sci.* **2011**, *4*, 3059. [CrossRef]
42. Serafin, J.; Dziejarski, B.; Cruz Junior, O.F.; Sreńscek-Nazzal, J. Design of Highly Microporous Activated Carbons Based on Walnut Shell Biomass for H_2 and CO_2 Storage. *Carbon* **2023**, *201*, 633–647. [CrossRef]
43. Ayawei, N.; Ebelegi, A.N.; Wankasi, D. Modelling and Interpretation of Adsorption Isotherms. *J. Chem.* **2017**, *2017*, 3039817. [CrossRef]
44. Myers, A.L.; Prausnitz, J.M. Thermodynamics of Mixed-Gas Adsorption. *AIChE J.* **1965**, *11*, 121–127. [CrossRef]
45. Herm, Z.R.; Swisher, J.A.; Smit, B.; Krishna, R.; Long, J.R. Metal−Organic Frameworks as Adsorbents for Hydrogen Purification and Precombustion Carbon Dioxide Capture. *J. Am. Chem. Soc.* **2011**, *133*, 5664–5667. [CrossRef] [PubMed]
46. Lu, W.; Yuan, D.; Sculley, J.; Zhao, D.; Krishna, R.; Zhou, H.-C. Sulfonate-Grafted Porous Polymer Networks for Preferential CO_2 Adsorption at Low Pressure. *J. Am. Chem. Soc.* **2011**, *133*, 18126–18129. [CrossRef] [PubMed]
47. Song, W.-C.; Xu, X.-K.; Chen, Q.; Zhuang, Z.-Z.; Bu, X.-H. Nitrogen-Rich Diaminotriazine-Based Porous Organic Polymers for Small Gas Storage and Selective Uptake. *Polym. Chem.* **2013**, *4*, 4690. [CrossRef]
48. Wang, J.; Krishna, R.; Yang, J.; Dandamudi, K.P.R.; Deng, S. Nitrogen-Doped Porous Carbons for Highly Selective CO_2 Capture from Flue Gases and Natural Gas Upgrading. *Mater. Today Commun.* **2015**, *4*, 156–165. [CrossRef]
49. Yue, L.; Xia, Q.; Wang, L.; Wang, L.; DaCosta, H.; Yang, J.; Hu, X. CO_2 Adsorption at Nitrogen-Doped Carbons Prepared by K2CO3 Activation of Urea-Modified Coconut Shell. *J. Colloid Interface Sci.* **2018**, *511*, 259–267. [CrossRef] [PubMed]
50. Serafin, J.; Baca, M.; Biegun, M.; Mijowska, E.; Kaleńczuk, R.J.; Sreńscek-Nazzal, J.; Michalkiewicz, B. Direct Conversion of Biomass to Nanoporous Activated Biocarbons for High CO_2 Adsorption and Supercapacitor Applications. *Appl. Surf. Sci.* **2019**, *497*, 143722. [CrossRef]
51. Samanta, A.; Zhao, A.; Shimizu, G.K.H.; Sarkar, P.; Gupta, R. Post-Combustion CO_2 Capture Using Solid Sorbents: A Review. *Ind. Eng. Chem. Res.* **2012**, *51*, 1438–1463. [CrossRef]
52. Kou, J.; Sun, L.-B. Fabrication of Nitrogen-Doped Porous Carbons for Highly Efficient CO_2 Capture: Rational Choice of a Polymer Precursor. *J. Mater. Chem. A* **2016**, *4*, 17299–17307. [CrossRef]